Electronic Supplementary Material (ESI) for Physical Chemistry Chemical Physics.
This journal is © the Owner Societies 2018

Supporting Information

Coexistence of distinct intramolecular electron transfer pathways in polyoxometalate based molecular triads

Yusen Luo[1,2], Maria Wächtler[2], Kevin Barthelmes[3,4], Andreas Winter[3,4], Ulrich S. Schubert[3,4] and Benjamin Dietzek*[1,2,4]

[1]*Institute of Physical Chemistry and Abbe Center of Photonics, Friedrich Schiller University Jena, Helmholtzweg 4, 07743 Jena, Germany*

[2]*Department Functional Interfaces, Leibniz Institute of Photonic Technology (IPHT), Albert-Einstein-Str. 9, 07745 Jena, Germany*

[3]*Laboratory of Organic and Macromolecular Chemistry (IOMC), Friedrich Schiller University Jena, Humboldtstr. 10, 07743 Jena, Germany*

[4]*Center for Energy and Environmental Chemistry Jena (CEEC Jena), Friedrich Schiller University Jena, Philosophenweg 7a, 07743 Jena, Germany*

**Corresponding author: benjamin.dietzek@leibniz-ipht.de*

Table of contents

General methods

The synthesis, electrochemistry and steady-state absorption and emission spectra of the mono-ruthenium complex, dyads and triads have been reported.[1-3] Steady-state UV/Vis absorption spectra (Figure S1a) and emission spectra (Figure S1b) collected in dimethyl sulfoxide (DMSO) are summarized for convenience. Steady-state UV/Vis absorption spectra were recorded with a JASCO V-670 spectrophotometer in a quartz cell with 1 mm path length. Steady-state emission spectra (λ_{ex} = 520 nm, optical density of each sample was adjusted to 0.1 at 520 nm) were recorded with a fluorescence spectrometer (Fluorolog, Horiba group) in a 1 cm quartz cell. For the time-resolved experiments and resonance Raman measurements the stability of samples was ensured by recording the steady-state UV/Vis absorption spectra before and after every measurement.

Electrochemistry. CV measurement for **PTZ-Ru** was carried out with PC-controlled potentiostat (VersaSTAT 3) with a standard three-electrode system by using a glassy-carbon-disk working electrode, a platinum wire counter electrode and an Ag/AgCl reference electrode. The scan rate is 200 mV/s. All potentials given in the manuscript refer to ferrocene as standard. Because of the limited electrochemical window of DMSO, the electrochemistry[1] was collected in dimethylformamide (DMF).

Time-Resolved Transient Absorption Spectroscopy. Femtosecond (fs) transient absorption (TA) spectra were collected by two different home-built pump-probe setups. Each setup is based on an amplified Ti: Sapphire oscillator (1 kHz, 800 nm).[4] The compounds were excited by pump pulses centered at 520 nm (TOPAS-C, Lightconversion Ltd.) with a duration of 80 fs. The power of the pump beam at the sample was kept at 0.45 mW, corresponding to an energy of 0.9 µJ per pump pulse. For measurements with a longer delay time range (up to 9.5 ns) the compounds were excited at 520 nm (TOPASwhite, Lightconversion Ltd.) with a duration of 110 fs. The power of the pump beam at the sample was kept at 0.3 mW, corresponding to an energy of 0.6 µJ per pump pulse. For both setups, a white light supercontinuum generated by focusing a fraction of the fundamental in a CaF_2 plate is used to probe the absorbance of the sample between 340 to 800 nm. The pump beam is delayed in time with respect to the probe beam by means of an optical delay line and the polarization between probe and pump is set at the magic angle (54.7°). Each sample solution (adjusted to yield an optical density of 0.2 at 520 nm) was kept in a 1 mm quartz cuvette. Transient absorption data were corrected for the chirp of the probe light and analyzed by a global multi-exponential fit after exclusion of a temporal window of 200 fs around time-zero in order to avoid contributions of the coherent-artifact region[5] to the data analysis.

Nanosecond (ns) TA spectra[2] were collected to study the lifetime of the long-lived species, which are visible in the fs TA data. The pump pulses centered at 520 nm were produced by a Continuum OPO Plus which is pumped by a continuum surelite Nd:YAG laser system (pulse duration 5 ns, repetition rate 10 Hz). The probe light is provided by a 75 W xenon arc lamp. Spherical concave mirrors are used to focus the probe beam into the samples and then to send the beam to the monochromator (Acton, Princeton Instruments). The spectrally selected probe light is detected by a Hamamatsu R928 photomultiplier. The signal is amplified and processed by a commercially available detection system (Pascher Instruments AB). Each sample was freshly prepared for the ns transient absorption measurements yielding an optical density of about 0.37 at the excitation wavelength, i.e. at 520 nm. All measurements were performed in 1 cm path length fluorescence cuvettes. For all measurements, the energy of the pump pulses was kept at 0.25 mJ. Oxygen-free solutions were realized by at least five freeze-pump-thaw cycles.

Resonance Raman Spectra. Excitation-wavelength dependent resonance Raman (rR) spectra were recorded in a conventional 90° scattering arrangement.[6] RR spectra were recorded upon excitation at 458, 476, 496 and 515 nm (delivered by a Coherent Innova300C MotoFreD Ion Laser). A rotating cell was utilized to prevent sample decomposition. In order to check for sample integrity, absorption spectra of the samples were recorded before and after each rR measurement. No changes in the absorption spectra were observed.

Considering the limited solubility of compounds studied in this manuscript, all spectroscopic experiments were performed upon dissolving the POM containing samples in DMSO.

Steady-state emission spectra

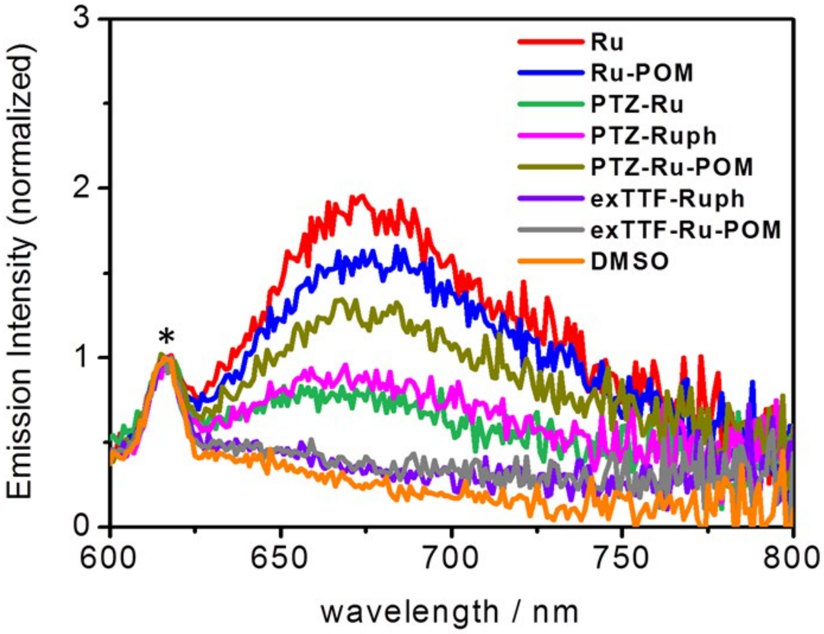

Figure S1. Normalized steady-state emission spectra (λ_{ex} = 520 nm, $OD_{520\ nm}$ = 0.1) of the compounds collected in aerated dimethyl sulfoxide (DMSO).[1,3] The emission spectra were normalized to the Raman band (asterisk) of the solvent DMSO.

Optimized molecular structure of PTZ-Ru-POM and exTTF-Ru-POM

The structures were optimized by molecular modelling (MM) with *BIOVIA* Material Studio v8.0 using the Forcite module with default settings (algorithm = smart; convergence tolerance: energy = 0.001 kcal/mol, force = 0.5 kcal/mol/Å; maximum number of iterations = 2000; motion groups rigid = NO). The start structure of the POM unit was the geometry optimized structure of a similar POM reported by Matt *et al.*.[7]

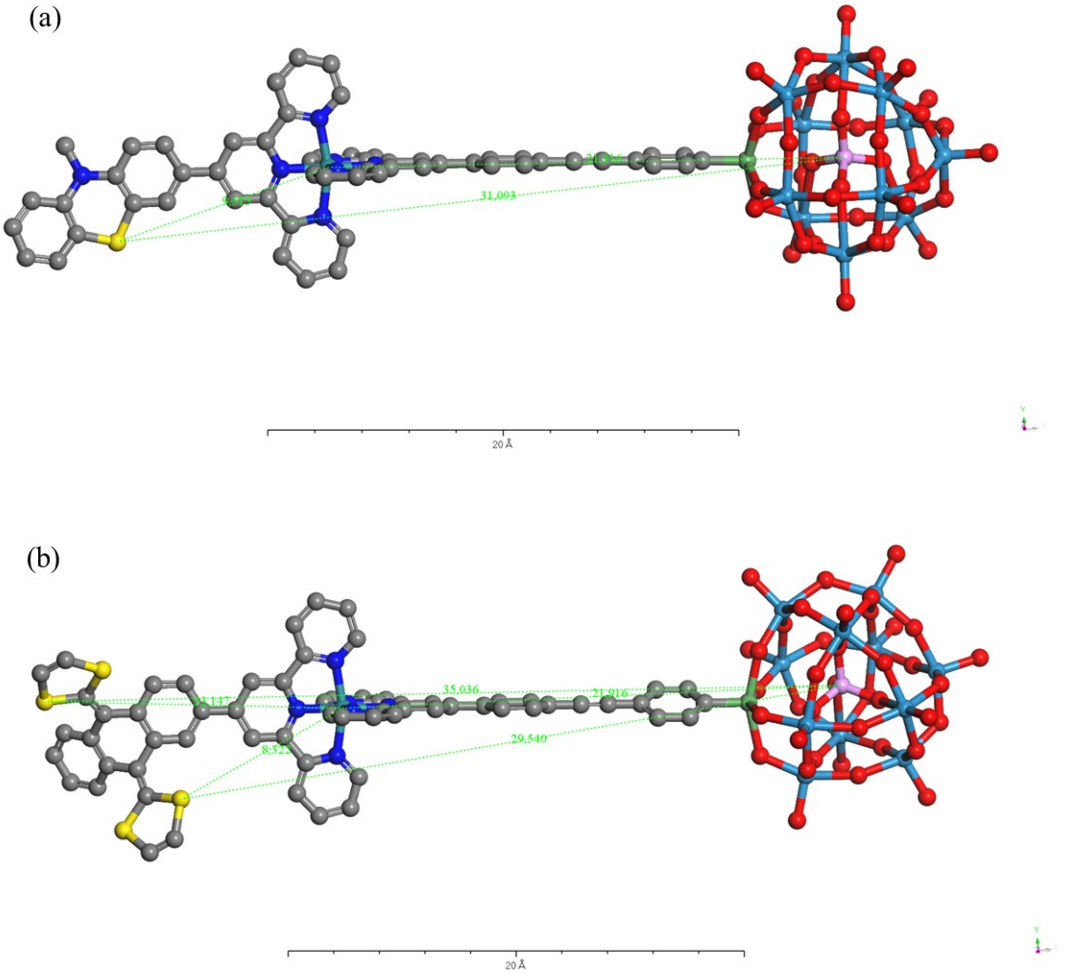

Figure S2. Optimized molecular structure of (a) **PTZ-Ru-POM** and (b) **exTTF-Ru-POM**. For measuring the center-to-center distance, the sulfur atom in PTZ and exTTF units, the ruthenium atom in Ru^{II} complex and the central phosphorus atom in POM were used. Since the exTTF unit has a butterfly-like shape and consists of four sulfur atoms, there are different distances from each sulfur atom. Only the shortest and longest distance were displayed and used.

Cyclic voltammetry curve of PTZ-Ru

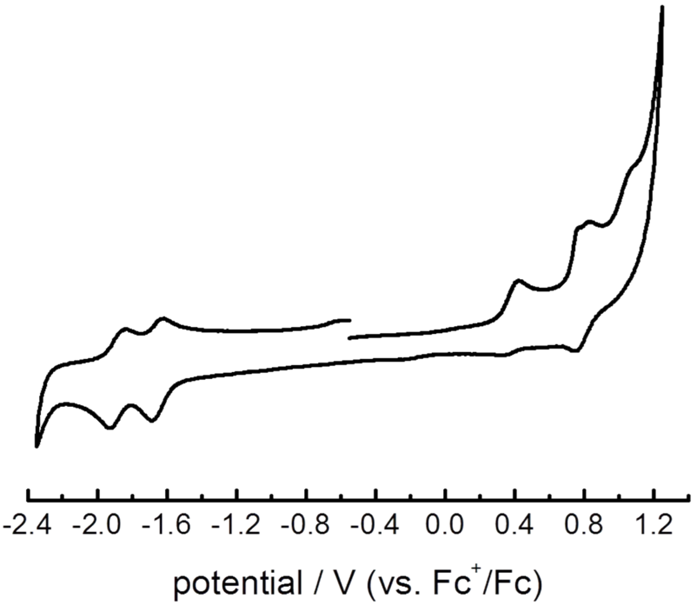

Figure S3. Cyclic voltammetry curve (scan rate 200 mV/s) for dyad **PTZ-Ru** in DMF/0.1 M Bu_4NPF_6.

Schematic illustration for the calculation of driving forces

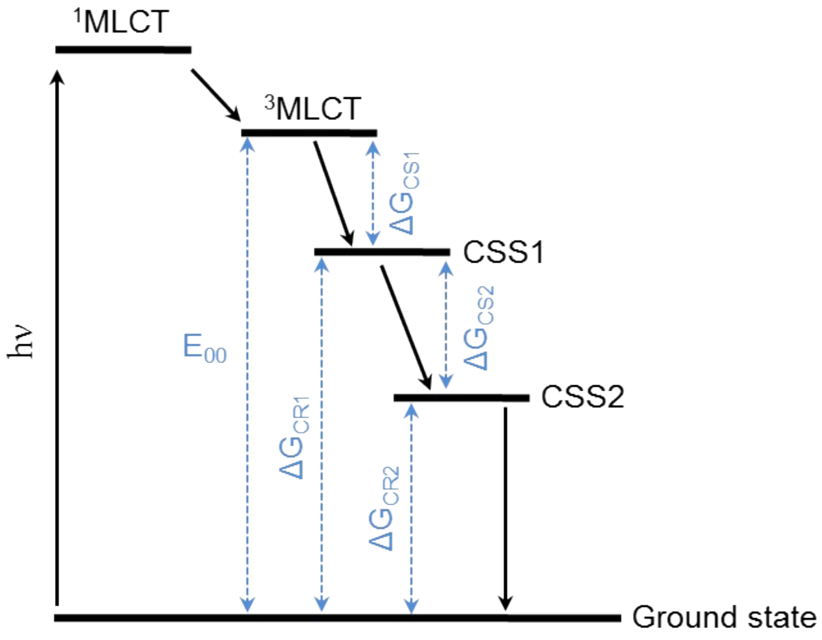

Scheme S1. The possible relaxation processes of the triads upon photoexcitation.

Here is an anticipated scheme for the two sequential electron-transfer processes of the triads after photoexcitation of the Ru-center. For the first charge separation (CSS1) the radical pairs are $tpy^{\cdot -}$ / $PTZ^{\cdot +}$ or $tpy^{\cdot -}$ / $exTTF^{\cdot +}$; for the second charge separation (CSS2) the radical pairs are $POM^{\cdot -}$ / $PTZ^{\cdot +}$ or $POM^{\cdot -}$ / $exTTF^{\cdot +}$, and $\Delta G^{\circ}_{CR} = e\,(E_{A/A^{-}} - E_{D^{+}/D}) + e^2 / 4\pi R\varepsilon_0\varepsilon_s$. $\Delta G^{\circ}_{CS1} = -\Delta G^{\circ}_{CR1} - E_{00}$ is the driving force for the first charge separation. E_{00} is the energy difference between the thermalized, lowest ^{3}MLCT excited state and ground state of Ru complex. Thus, the driving force for the second charge separation (*i.e.* from CSS1 to CSS2 state) can be calculated by $\Delta G^{\circ}_{CS2} = \Delta G^{\circ}_{CR1} - \Delta G^{\circ}_{CR2}$.

Driving forces in DMSO

According to the literature report,[8,9] the driving forces in DMSO can be calculated by the following equation:

$$\Delta G^{\circ}_{CS} = e\,(E_{D^{+}/D} - E_{A/A^{-}}) - E_{00} - \frac{e^2}{4\pi\varepsilon_0\varepsilon R_{DA}} - \frac{e^2}{8\pi\varepsilon_0}\left(\frac{1}{r_{D^{+}}} + \frac{1}{r_{A^{-}}}\right)\left(\frac{1}{\varepsilon_{ref}} - \frac{1}{\varepsilon}\right)$$

the last term concerning the difference of solvation free enthalpies in different solvents used in electrochemistry (ε_{ref}) and photo-physical measurement (ε). R_{DA} is the distance between donor and acceptor. r_{D}^{+} and r_{A}^{-} represent the radius of the oxidized donor and reduced acceptor, respectively.

Table S1. Estimated radii of neutral electron donors and acceptors.

unit	radius / Å^{a}	radius / Å^{b}
PTZ	3.7	3.6^{c}
exTTF	4.6	4.2^{d}
Ru complex	4.7	4.7^{e}
POM	6.2	5.3^{f}

[a] Radii of electron donors and acceptors were obtained from the optimized molecular structures shown in Figure S2 which were measured without considering the outside hydrogens. [b] Shows the comparison to the radii obtained from the crystal structures (without hydrogens). [c-f] Were taken from ref. 10-13.

Table S2. Center-to-center distances R, electrochemical data and reaction free-energy changes (–ΔG°) for charge separation (CS) and charge recombination (CR) in DMSO.

	center-to-center / Å		E° / V (vs Fc^{+}/Fc)^{e}				- ΔG° / eV^{f}			
	R$_{(D\text{-}Ru)}$^{a}	R$_{(D\text{-}POM)}$^{b}	D^{+}/D	Ru^{3+}/Ru^{2+}	POM/POM^{-}	tpy/tpy^{-}	CS1	CR1	CS2	CR2
PTZ-Ru	9.5	-	0.37	0.78	-	-1.65	0.10	1.97	-	-
PTZ-Ru-POM	9.5	31.1	0.29	0.75	-1.45	-1.69	0.14	1.93	0.22	1.71
exTTF-Ruph	8.3^{c} (13.2)^{d}	-	-0.16	0.84	-	-1.55	0.73^{c} (0.72)^{d}	1.34^{c} (1.35)^{d}	-	-
exTTF-Ru-POM	8.3^{c} (13.2)^{d}	29.5^{c} (35.0)^{d}	-0.30	0.84	-1.46	-1.63	0.79^{c} (0.78)^{d}	1.28^{c} (1.29)^{d}	0.14^{c} (0.15)^{d}	1.14^{c} (1.14)^{d}

[a,b] Center-to-center distances (Figure S2) between the electron donor (PTZ or exTTF) and Ru^{II} complex ($R_{D\text{-}Ru}$) or POM ($R_{D\text{-}POM}$). [c] Shortest and [d] longest distance between exTTF and Ru^{II} complex since the exTTF unit has a butterfly-like shape and consists of four sulphur atoms (Figure S2b). [e] Except **PTZ-Ru** (Figure S3), redox potentials were taken from ref. 1. [f] driving forces for charge-separation and charge-recombination in DMSO were calculated by the equation shown above which concerning the different solvents used in electrochemistry and photo-physical measurement. For calculation, the radii of neutral electron donors and acceptors obtained from the optimized molecular structures were used (Table S1).

fs TA spectra of PTZ-Ru and PTZ-Ru-POM at longer time scale

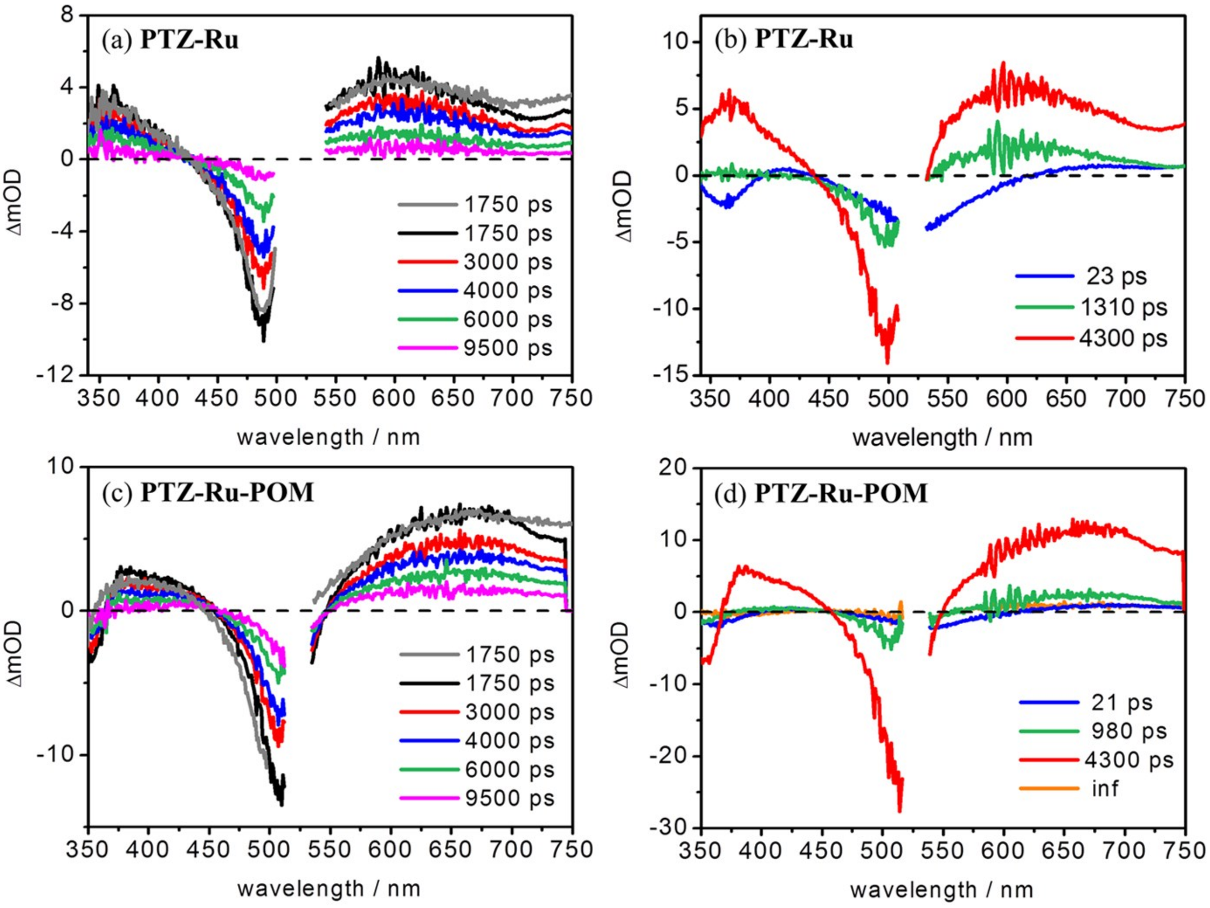

Figure S4. Femtosecond (fs) transient absorption (TA) spectra at selected times of (a) **PTZ-Ru** and (c) **PTZ-Ru-POM** upon excitation at 520 nm in aerated DMSO in the time range of 1750 to 9500 ps. To combine the fs TA data collected by a short and a long optical delay line, the spectra were scaled according to the spectrum obtained by the short delay line at 1750 ps at 590 and 680 nm (grey solid line) for **PTZ-Ru** and **PTZ-Ru-POM**, respectively. (b) and (d) Corresponding decay-associated spectra which were obtained by fixing the first two time constants obtained from the fs TA data measured with a short optical delay line.

ns TA spectra of PTZ-Ru and PTZ-Ruph

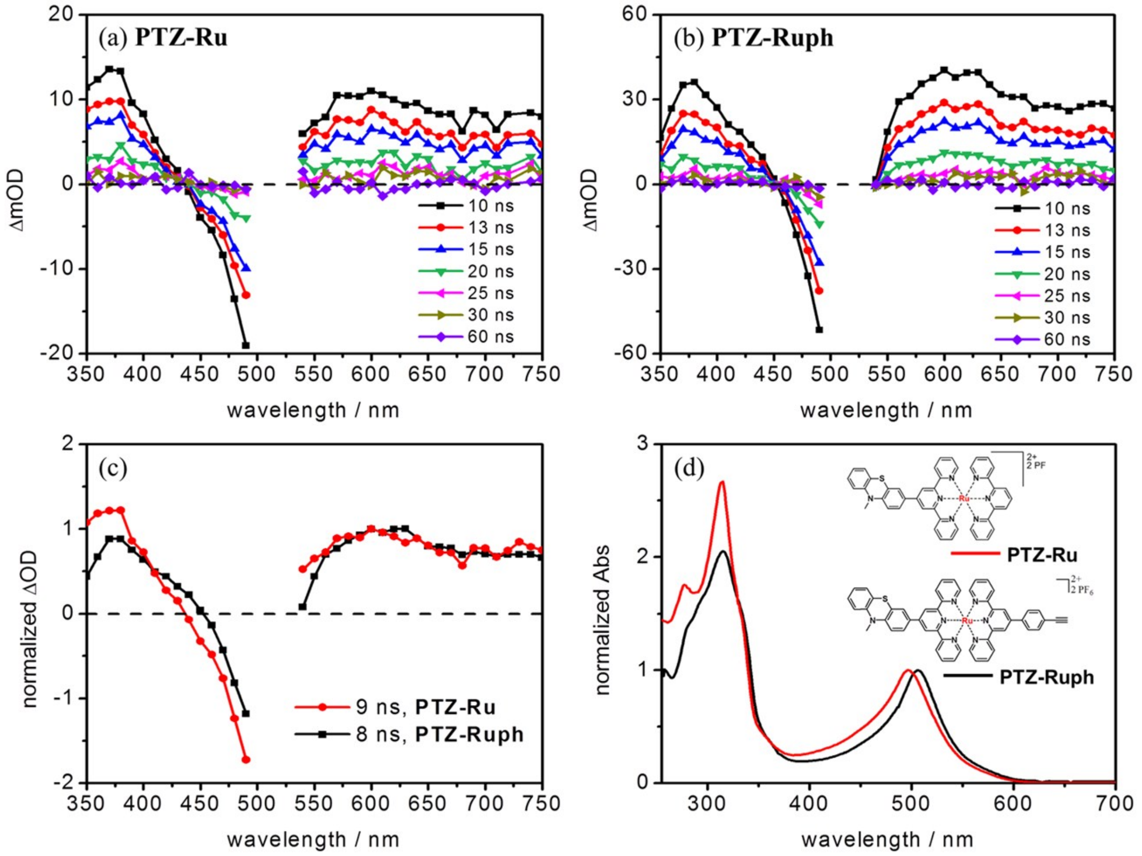

Figure S5. Nanosecond (ns) transient absorption (TA) spectra at selected times of (a) **PTZ-Ru** and (b) **PTZ-Ruph** upon excitation at 520 nm in aerated DMSO. (c) Normalized (at 600 nm) global fit result of the ns TA. (d) Normalized (at absorption maximum for each compound) UV/Vis absorption spectra in DMSO.

fs TA spectra of Ru-POM

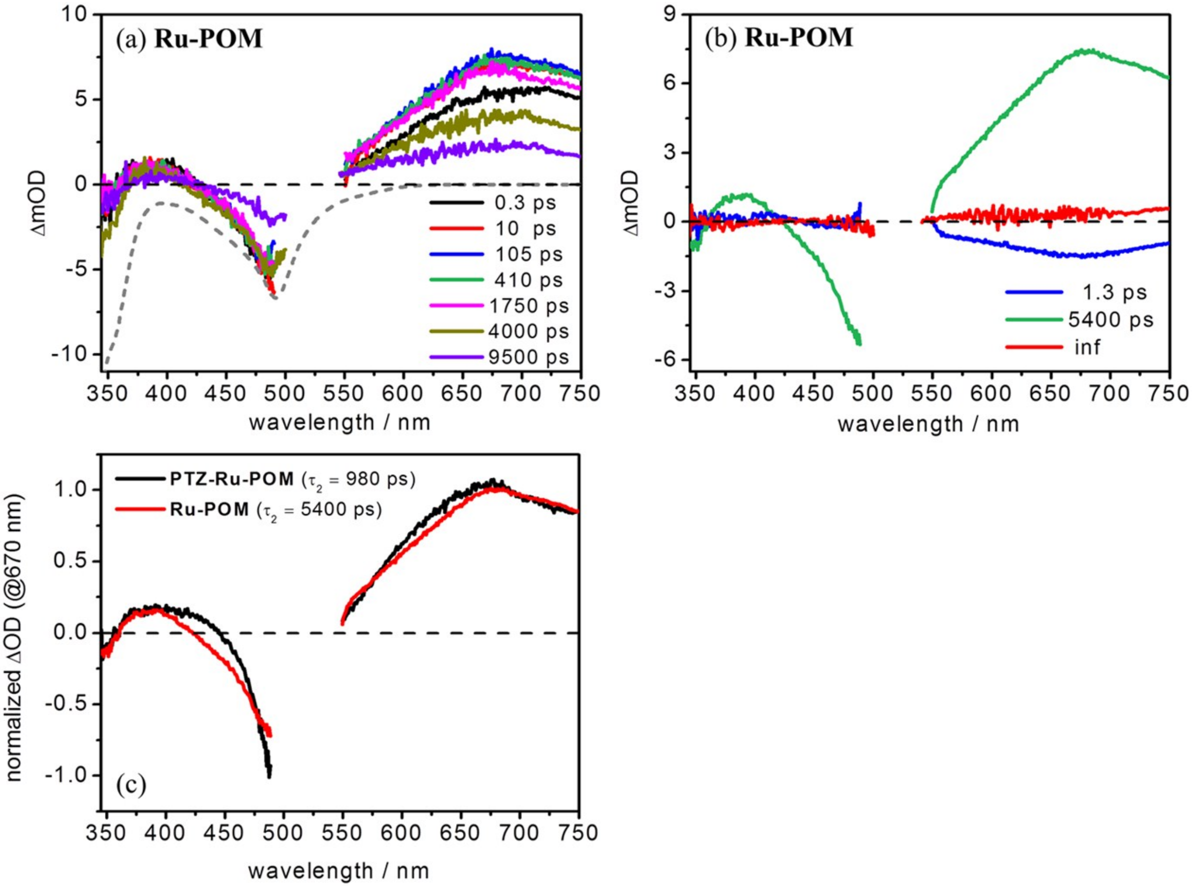

Figure S6. (a) Femtosecond transient absorption spectra at selected times of (a) **Ru-POM** upon excitation at 520 nm in aerated DMSO and (b) decay-associated spectra.[3] (c) Comparison of the second species (normalized at 670 nm) in decay-associated spectra of **PTZ-Ru-POM** (see the main text) and **Ru-POM**.

ns TA spectra of PTZ-Ru-POM

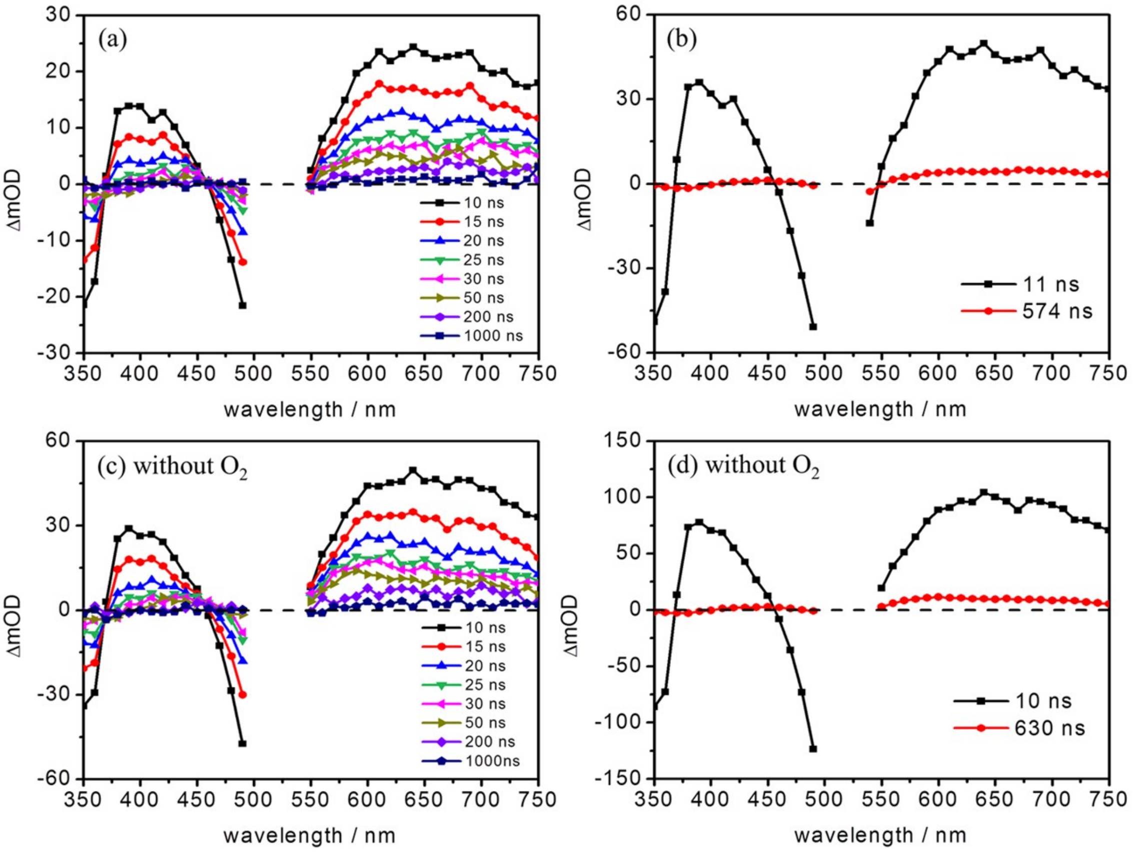

Figure S7. Nanosecond (ns) transient absorption (TA) spectra at selected times of **PTZ-Ru-POM** upon excitation at 520 nm in (a) aerated and (c) deaerated DMSO. (b) and (d) Corresponding global fit results of the ns TA data. Note: the time constant for the first species (~10 ns) obtained from the global fit is close to the time resolution of our setup. In order to get a more reliable value for this process fs TA spectra with a longer delay line (~9.5 ns) was used (see Figure S4).

Integrated kinetic trace of the ns TA data of PTZ-Ru-POM

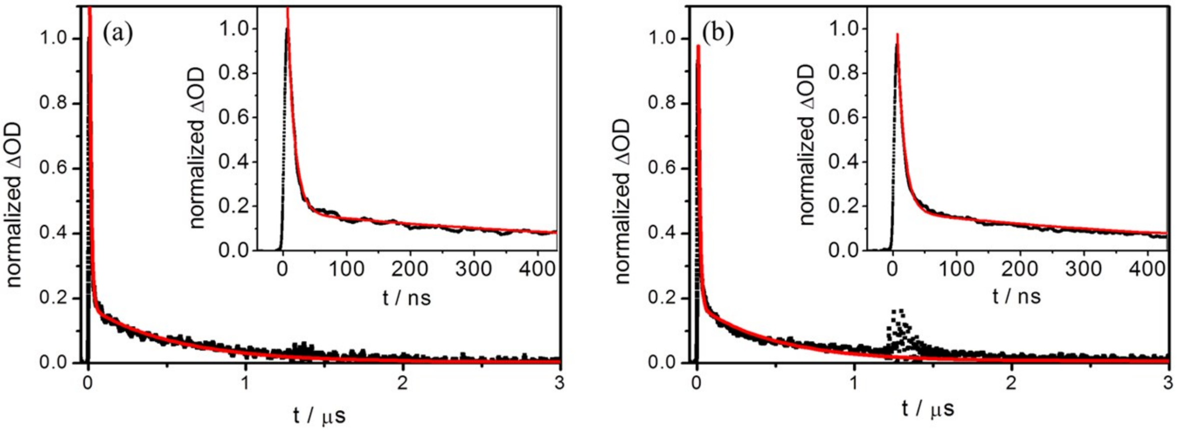

Figure S8. Normalized integrated kinetic trace at the spectral region between 540 and 750 nm where shows significant absorption signals of both species in ns TA data of **PTZ-Ru-POM** collected upon excitation at 520 nm in (a) aerated and (b) deaerated DMSO. Inset: the enlargement of the time region up to 425 ns. The decay was fitted by a bi-exponential function: $I\ (x) = A_1 \cdot \exp(-x/\tau_1) + A_2 \cdot \exp(-x/\tau_2) + I_0$.

Simulation of the absorption spectra of the oxidized donor in PTZ-Ru-POM

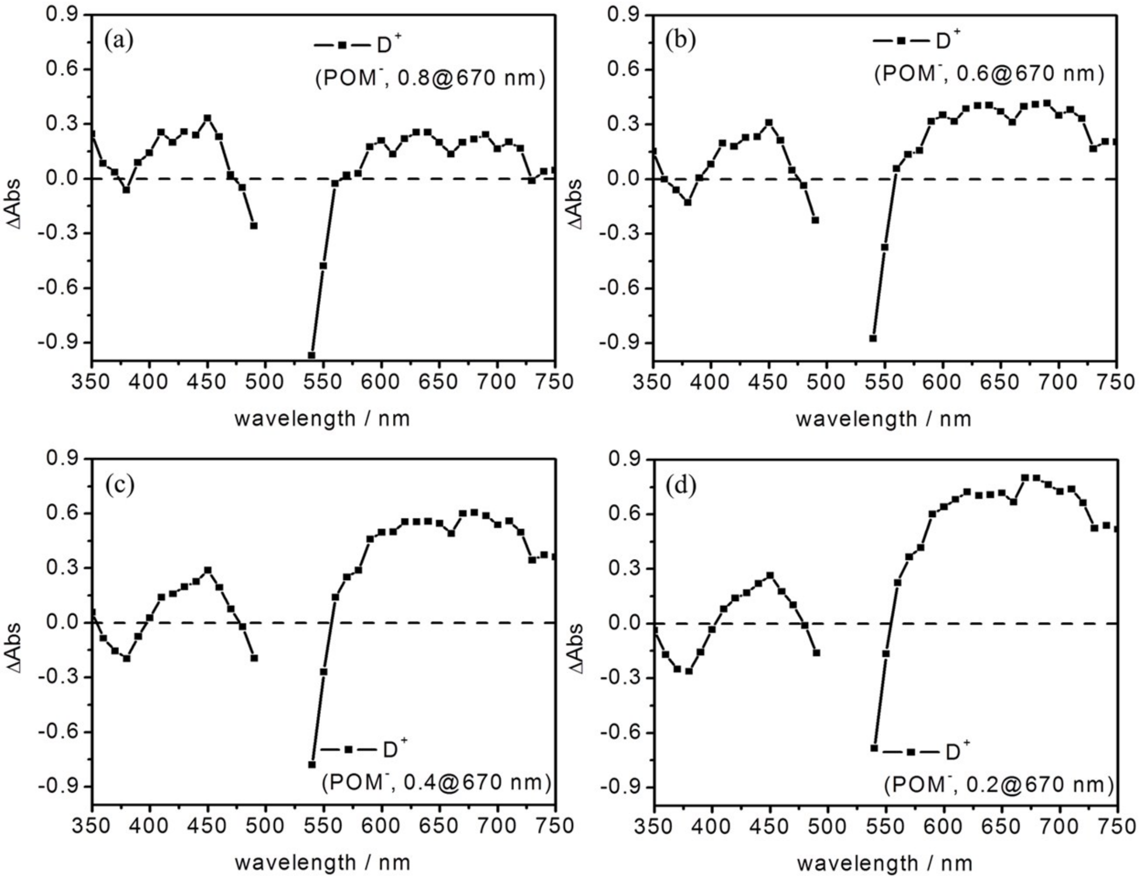

Figure S9. In order to exclude the formation of PTZ$^{\cdot+}$-Ru(tpy)$_2$-POM$^{\cdot-}$, the absorption spectra of the oxidized donor (D$^+$) were simulated: from the normalized (at 670 nm) spectrum of the long-lived species in global fit of the ns TA data (Figure S7b) different contributions of the reduced POM were subtracted. The POM$^{\cdot-}$ has a contribution at 670 nm of (a) 0.8, (b) 0.6, (c) 0.4 and (d) 0.2. All the resulting spectra do not display the significant positive absorption bands of PTZ$^{\cdot+}$ at 365, 470 and 590 nm.[14,15] Thus the long-lived species in **PTZ-Ru-POM** is not the PTZ$^{\cdot+}$-Ru(tpy)$_2$-POM$^{\cdot-}$. See Figure S10a for the spectrum of reduced POM.

Comparison of the sub-μs species ns TA data with the SEC results

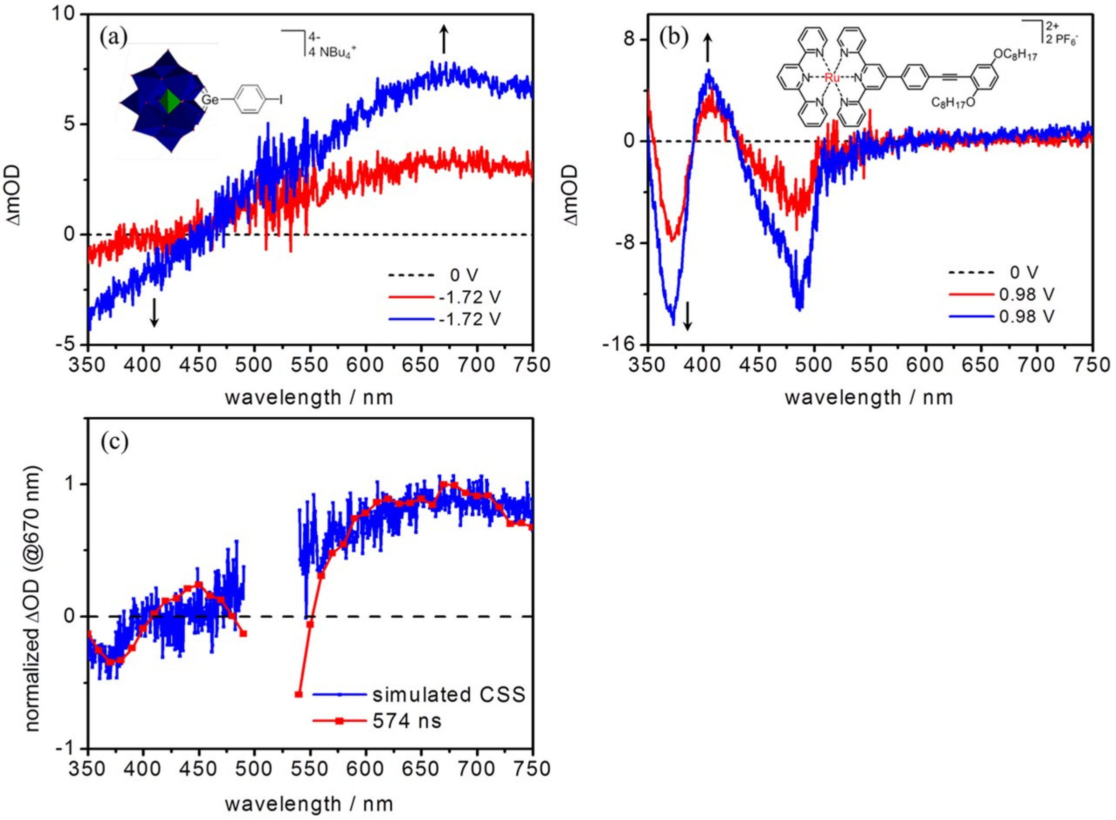

Figure S10. (a) Reductive and (b) oxidative spectroelectrochemistry-UV/Vis absorption difference spectra of POM and Ru, respectively.[3] Inset: molecular structure of the POM and Ru complex studied. (c) Comparison of the long-lived species in global fit results of the ns TA data of **PTZ-Ru-POM** with the simulated spectrum of Ru^{III}-$\text{POM}^{\cdot -}$ taken from ref. 3.

Resonance Raman spectra of PTZ-Ru-POM

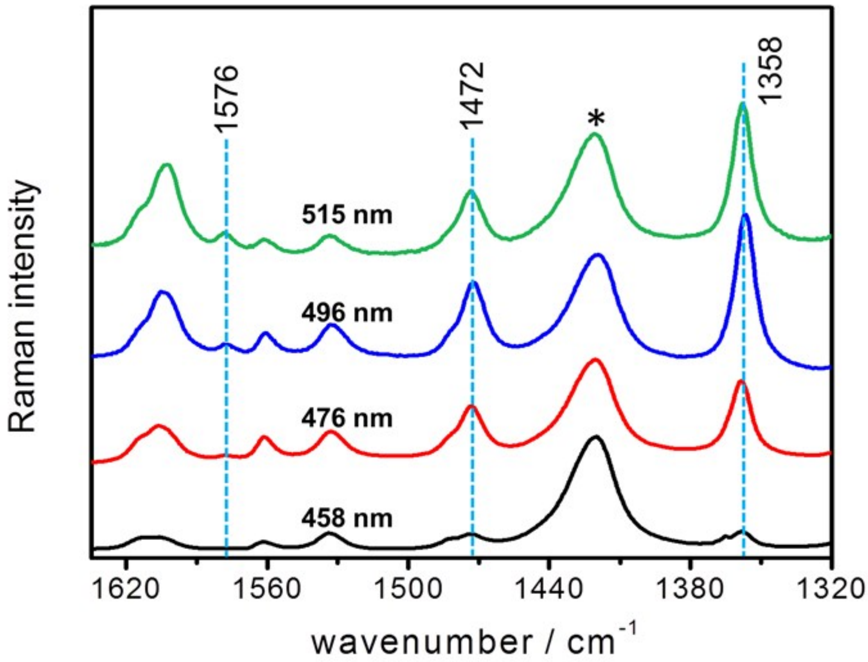

Figure S11. Resonance Raman spectra of **PTZ-Ru-POM** recorded in DMSO with excitation wavelengths at 515, 496, 476 and 458 nm. For comparison the spectra were normalized to the solvent band (asterisks) at 1420 cm^{-1} and only the modes (associated with PTZ) showing distinct differences in signal intensities upon variation of the excitation wavelengths were marked.

The excitation-wavelength dependent resonance Raman of triad **PTZ-Ru-POM** shows similar results to that of **PTZ-Ru**.[14] Thus the Jablonski scheme for **PTZ-Ru-POM** was made by referring to **PTZ-Ru**.[14]

Comparison of the fs TA spectra of exTTF-Ruph and Ruph

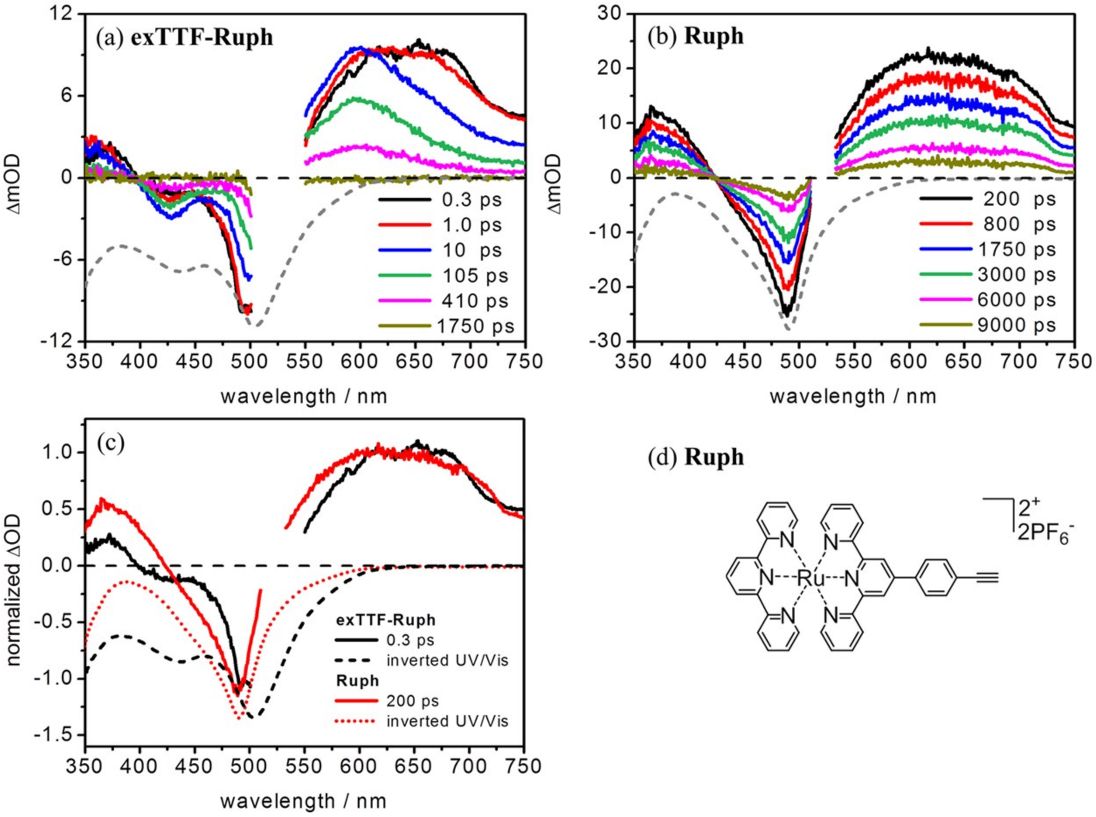

Figure S12. Femtosecond (fs) transient absorption (TA) spectra at selected times of (a) **exTTF-Ruph** (short optical delay line) and (b) **Ruph** (long optical delay line) upon excitation at 520 nm in aerated DMSO. The grey dashed line in a and b represents the inverted ground state absorption spectrum respectively. (c) Comparison of the spectrum of **exTTF-Ruph** collected at 0.3 ps and **Ruph** collected at 200 ps. (d) Molecular structure of **Ruph** studied.

For the mono-ruthenium complex **Ruph**, the transient absorption spectra collected at long delay times, e.g. 200 ps, shows the decay of the ^{3}MLCT state. The spectral features of **exTTF-Ruph** collected at early times, i.e. 0.3 ps, resemble the spectrum of the ^{3}MLCT state in **Ruph** but with a slight red-shift which is already indicated in the inverted UV/Vis absorption spectra (Figure S12c).

fs TA spectra of exTTF-Ru-POM at longer time scale

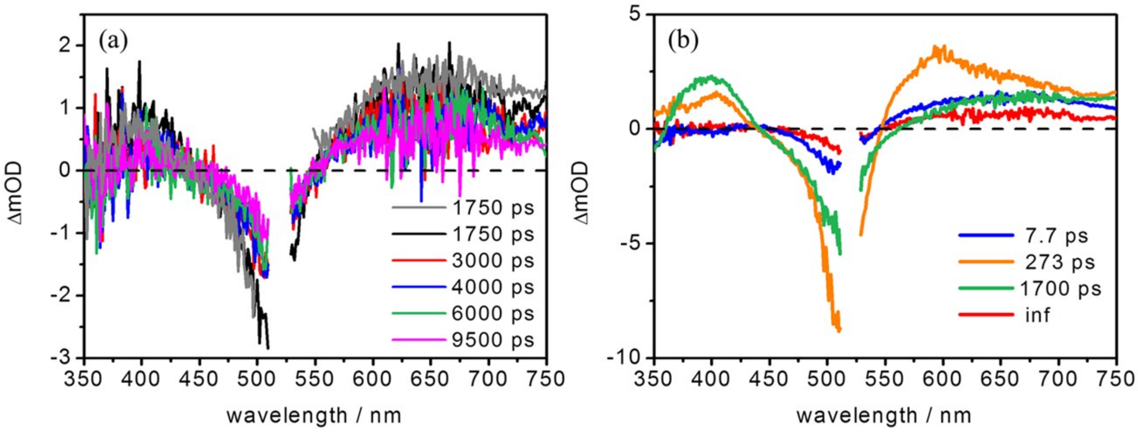

Figure S13. (a) Femtosecond (fs) transient absorption (TA) spectra at selected times of **exTTF-Ru-POM** upon excitation at 520 nm in aerated DMSO in the time range of 1750 to 9500 ps. To combine the fs TA data collected by a short and a long optical delay line, the spectra were scaled according to the spectrum obtained by the short delay line at 1750 ps at 630 nm (grey solid line). (b) Corresponding decay-associated spectra which were obtained by fixing the first two time constants obtained from the fs TA data measured with a short optical delay line.

ns TA spectra of exTTF-Ru-POM

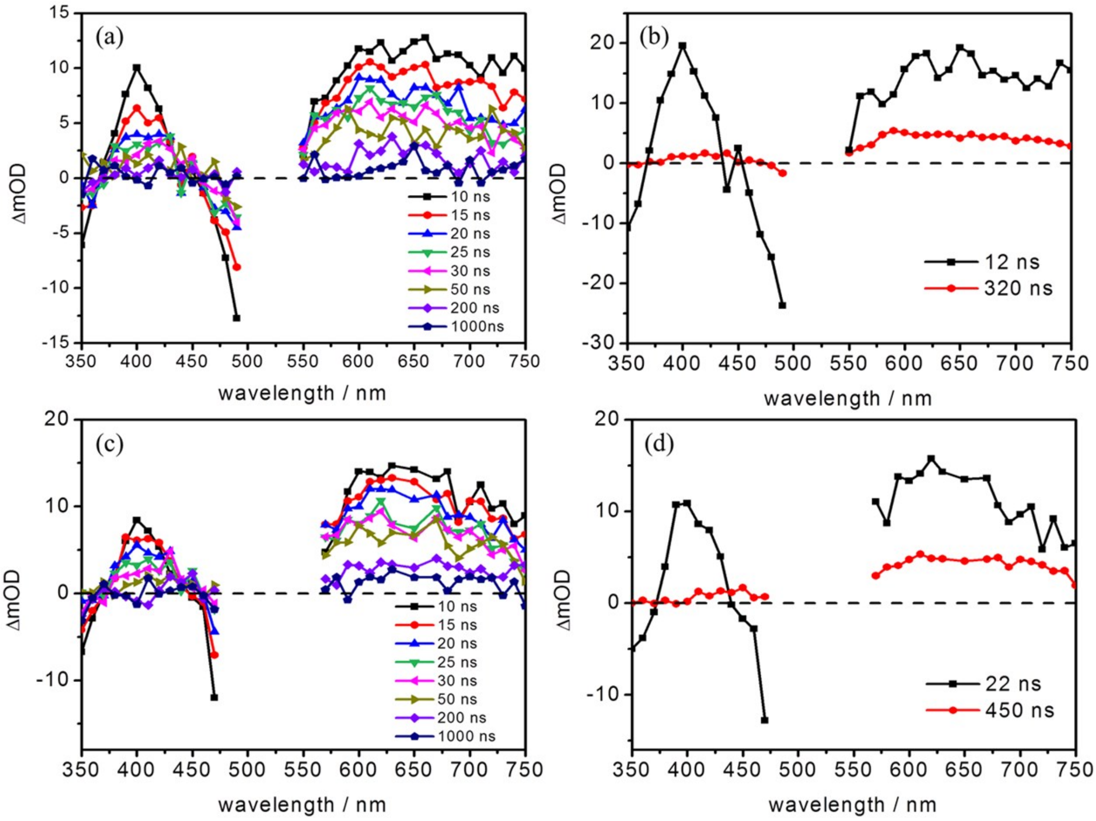

Figure S14. Nanosecond (ns) transient absorption (TA) spectra at selected times of **exTTF-Ru-POM** upon excitation at 520 nm in (a) aerated and (c) deaerated DMSO. (b) and (d) Corresponding global fit results of the ns TA data. Note: the time constant for the first species obtained from the global fit is close to the time resolution of our setup. In order to get the accurate value for this process fs TA spectra with a longer delay line (~9.5 ns) was used (see Figure S13).

Integrated kinetic trace of the ns TA data of exTTF-Ru-POM

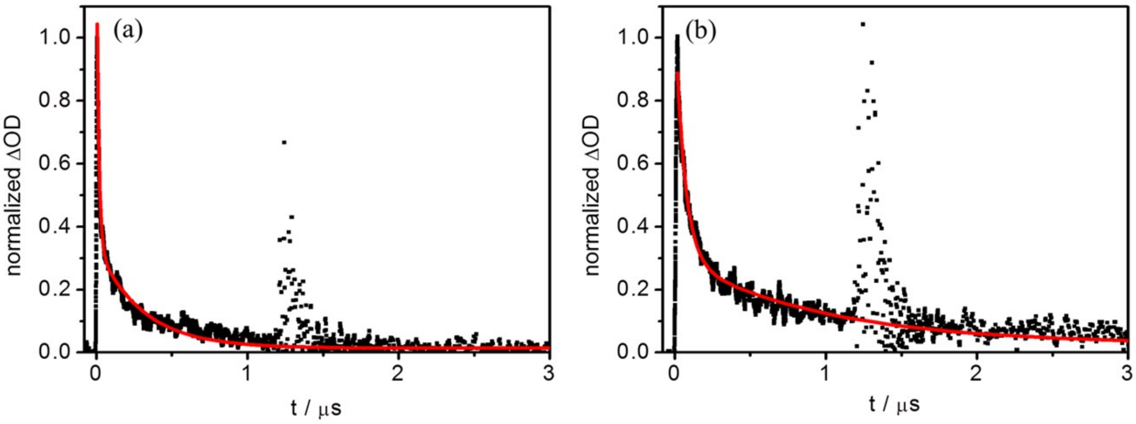

Figure S15. Normalized integrated kinetic trace at the spectral region between 540 and 750 nm of **exTTF-Ru-POM** collected upon excitation at 520 nm in (a) aerated and (b) deaerated DMSO.

Jablonski scheme for PTZ-Ru

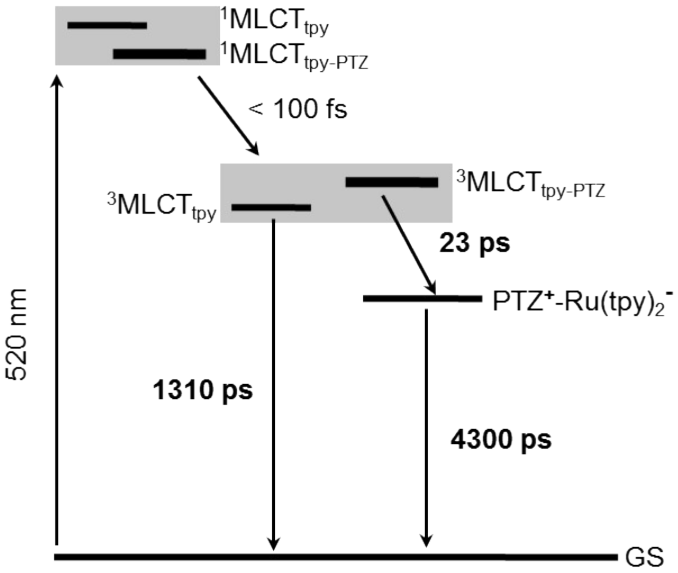

Scheme S2. Photoinduced relaxation processes for **PTZ-Ru**.

References

1 K. Barthelmes, M. Sittig, A. Winter, U. S. Schubert, *Eur. J. Inorg. Chem.* 2017, **2017**, 3698–3706.

2 K. Barthelmes, J. Kübel, A. Winter, M. Wächtler, C. Friebe, B. Dietzek, U. S. Schubert, *Inorg. Chem.* 2015, **54**, 3159–3171.

3 Y. Luo, M. Wächtler, K. Barthelmes, A. Winter, U. S. Schubert, B. Dietzek, *Chem. Commun.* 2018, DOI: 10.1039/c7cc09181h.

4 J. Kübel, R. Schroot, M. Wächtler, U. S. Schubert, B. Dietzek, M. Jäger, *J. Phys. Chem. C* 2015, **119**, 4742–4751.

5 B. Dietzek, T. Pascher, V. Sundström, A. Yartsev, *Laser Phys. Lett.* 2007, **4**, 38–43.

6 L. Zedler, J. Guthmuller, I. R. Moraes, S. Kupfer, S. Krieck, M. Schmitt, J. Popp, S. Rau, B. Dietzek, *Chem. Commun.* 2014, **50**, 5227–5229.

7 B. Matt, X. Xiang, A. L. Kaledin, N. Han, J. Moussa, H. Amouri, S. Alves, C. L. Hill, T. Lian, D. G. Musaev, G. Izzeta, A. Proust, *Chem. Sci.* 2013, **4**, 1737–1745.

8 D. Rehm, A. Weller, *Isr. J. Chem.* 1970, **8**, 259–271.

9 A. Weller, *Z. Phys. Chem.* 1982, **133**, 93–98.

10 S. S.C. Chu, D. V. D. Helm, *Acta Cryst.* 1974, **B30**, 2489–2490.

11 Y. Ren, S. Lee, J. A. Bertke, J. S. Moore, *Acta Crys. Sect. E* 20[15], **71**, 1475–1479.

12 E. C. Constable, C. E. Housecroft, E. A. Medlycott, M. Neuburger, F. Reinders, S. Reymann, S. *Inorg. Chem. Commun.* 2008, **11**, 805–808.

13 E. V. Radkov, R. H. Beer, *Inorg. Chim. Acta* 2000, **297**, 191–198.

14 Y. Luo, K. Barthelmes, M. Wächtler, A. Winter, U. S. Schubert, B. Dietzek, *Chem. Eur. J.* 2017, **23**, 4917–4922.

15 Y. Luo, K. Barthelmes, M. Wächtler, A. Winter, U. S. Schubert, B. Dietzek, *J. Phys. Chem. C* 2017, **121**, 9220–9229.